scientific reports

Check for updates

OPEN

Network toxicology, transcriptomics, and cytotoxic validation reveal TDCPP-induced pterygium mechanisms

Ji Yang[1,4], Jiajie Li[1,4], Boyu Liang[1,4], Nishan Zhao[2,4], Peng Zhang[1], ChengYan Fang[1], Tao Xie[1], Ping Xiang[3]✉ & Hai Liu[1]✉

Pterygium, a common ocular surface disorder, is associated with environmental factors such as ultraviolet exposure and air pollution. Tris(1,3-dichloro-2-propyl) phosphate (TDCPP), a widely used organophosphate flame retardant, has been detected in environmental and biological samples, yet its role in pterygium pathogenesis remains unclear. This study employed an integrative approach combining network toxicology, transcriptome sequencing, and in vitro cytotoxicity assays to elucidate the molecular mechanisms linking TDCPP exposure to pterygium development. Bioinformatics analysis identified 273 TDCPP-related targets and 1,078 pterygium-associated genes, with 43 overlapping candidates. Weighted gene co-expression network analysis (WGCNA) revealed two key modules correlated with pterygium phenotypes, highlighting *MMP3* as a central regulator. Molecular docking and dynamics simulations confirmed stable interactions between TDCPP and *MMP3* (binding energy: -5.9 kcal/mol), supported by RMSD, RMSF, and hydrogen bonding analyses. In vitro experiments demonstrated that low-dose TDCPP (0.5 μM) upregulated *MMP3* expression in immortalized human conjunctival fibroblasts, enhancing cell proliferation, while higher concentrations (50 μM) induced cytotoxicity. These findings suggest that TDCPP promotes pterygium pathogenesis via MMP3-mediated extracellular matrix remodeling and fibroblast proliferation. This study provides novel insights into the environmental etiology of pterygium and identifies *MMP3* as a potential therapeutic target for TDCPP-associated ocular surface disorders.

Keywords Pterygium, TDCPP, MMP3, Network toxicology, Transcriptomics, Cytotoxicity

Pterygium is a common ocular surface disorder characterized by the abnormal growth of fibrovascular tissue from the conjunctiva onto the cornea, affecting approximately 12% of the global population with higher prevalence in tropical and subtropical regions[1,2]. This condition can lead to visual impairment, chronic irritation, and cosmetic concerns, significantly impacting patients' quality of life[3]. Although surgical excision remains the primary treatment, recurrence rates remain high (15.8–37%), underscoring the need for better understanding of its pathogenesis and preventive strategies[4,5].

The etiology of pterygium is multifactorial, involving genetic predisposition, chronic ultraviolet (UV) exposure, and environmental pollutants[6,7]. Mounting evidence suggests that airborne contaminants, including organophosphate flame retardants (OPFRs), may contribute to ocular surface diseases[8,9]. Among OPFRs, tris(1,3-dichloro-2-propyl) phosphate (TDCPP) is widely used in consumer products due to its flame-retardant properties and has been detected in indoor dust and biological samples[10,11]. In a study on household dust conducted in Japan, the median concentration of TDCPP (Tris(1,3-dichloro-2-propyl) phosphate) detected in floor dust was 8.69 μg/g, while the median concentration in multi-surface dust was 25.8 μg/g[12]. Additionally, in household dust from the Midwestern region of the United States, the median concentration of its metabolite BDCIPP (Bis(1,3-dichloro-2-propyl) phosphate) was 234 ng/g[13]. TDCPP exposure has been linked to systemic

[1]Department of Ophthalmology, The Eye Disease Clinical Medical Research Center of Yunnan Province, the Eye Disease Clinical Medical Center of Yunnan Province, The Second People's Hospital of Yunnan Province, Affiliated Hospital of Yunnan University, Kunming, China. [2]Department of Pathology, Affiliated Hospital of Yunnan University, Kunming, China. [3]Institute of Environmental Remediation and Human Health, School of Ecology and Environment, Southwest Forestry University, Kunming, China. [4]Ji Yang, Jiajie Li, Boyu Liang and Nishan Zhao contributed equally to this work. ✉email: xiangping@swfu.edu.cn; herryhai@ynu.edu.cn

toxicity, including neurodevelopmental disorders, endocrine disruption, and oxidative stress[14,15]. Notably, our previous studies demonstrated that OPFRs like TDCPP can induce corneal epithelial damage, suggesting potential ocular toxicity[16,17]. In Yunnan, China, where indoor TDCPP levels are elevated, pterygium prevalence reaches 22.6–35.27% in adults over 40 years[18]., yet the mechanistic role of TDCPP in pterygium remains unexplored.

Pathologically, pterygium involves fibroblast proliferation, extracellular matrix (ECM) remodeling, and chronic inflammation, with matrix metalloproteinases (MMPs) playing a key role[19]. MMP3, in particular, is overexpressed in pterygium tissues and implicated in ECM degradation and fibrovascular growth[20]. However, whether TDCPP modulates MMP3 or other molecular pathways to drive pterygium development is unknown. Addressing this gap requires integrative strategies combining computational predictions with experimental validation.

Here, we employed a multi-omics approach to investigate TDCPP's role in pterygium. Using network toxicology, we identified shared targets between TDCPP and pterygium, followed by transcriptome sequencing of clinical samples to pinpoint dysregulated genes. Weighted gene co-expression network analysis (WGCNA) revealed critical gene modules, while molecular docking and dynamics simulations characterized TDCPP-MMP3 interactions. In vitro assays using immortalized conjunctival fibroblasts validated TDCPP's dose-dependent effects on MMP3 expression and cell proliferation. Figure 1 depicts our research protocol. Our study bridges environmental exposure data with molecular mechanisms, offering insights into TDCPP as a risk factor for pterygium and highlighting MMP3 as a potential therapeutic target.

Materials and methods

Visual overview of the study process

Figure 1 offers a flowchart that provides a clear depiction of the study's procedural steps. For your convenience, supplementary file contains an exhaustive inventory of all the database resources utilized in this research, complete with their corresponding access links.

Unveiling TDCPP targets: database-driven identification

The chemical composition of Tris(1,3-dichloro-2-propyl) phosphate (TDCPP) was obtained from the PubChem database. Potential targets of TDCPP in Homo sapiens were identified using databases including Super-Pred (URL: https://prediction.charite.de/subpages/target_prediction.php), ChEMBL (URL: https://www.ebi.ac.uk/chembl/), STITCH (URL: http://stitch.embl.de/), and PharmMapper (URL: https://www.lilab-ecust.cn/pharmmapper/)[21–23].

Deciphering pterygium-related targets: overlap analysis with TDCPP targets

Pterygium-associated target genes were retrieved from Genecards (URL: https://www.genecards.org/) and OMIM (URL: https://www.omim.org/). The overlap between pterygium-related targets and those of Tris(1,3-dichloro-2-propyl) phosphate (TDCPP) was identified, indicating potential targets for TDCPP-induced pterygium toxicity.

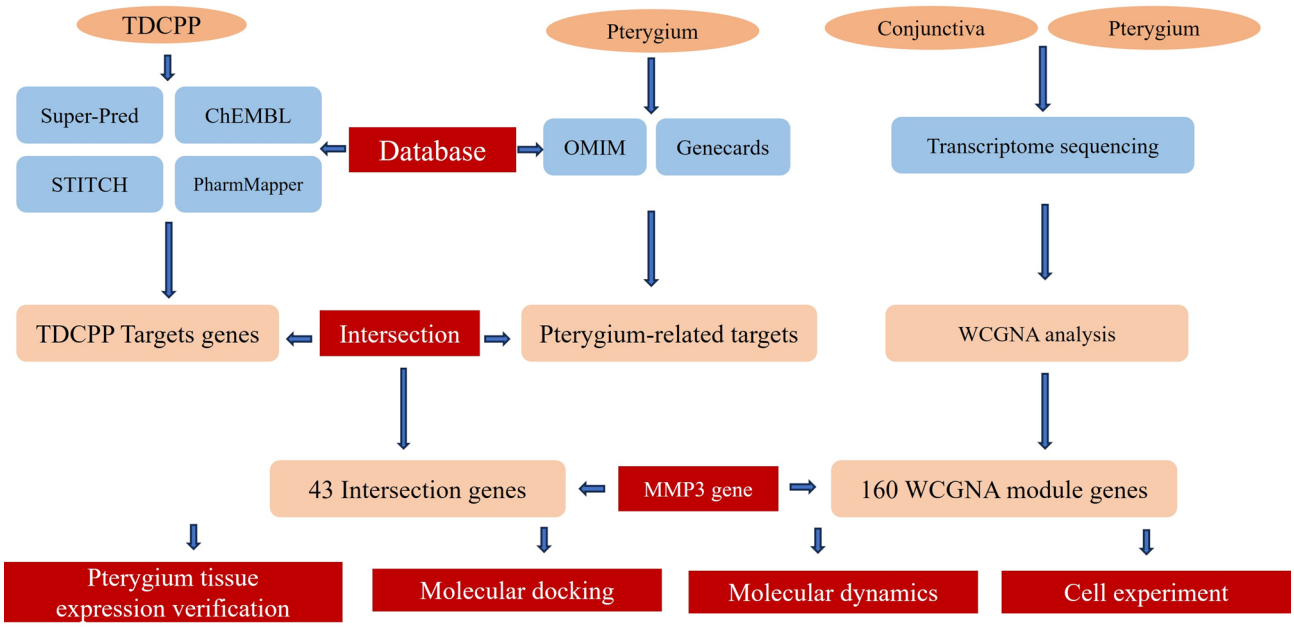

Fig. 1. Research Design Flow Chart.

Analysis of target proteins for gene function and pathway enrichment

We utilized the version 4.2.1 of the R project 'clusterProfiler' R package[24] to conduct Gene Ontology (GO) and Kyoto Encyclopedia of Genes and Genomes (KEGG) analyses on potential targets in TDCPP-induced pterygium[25]. The GO analysis examined biological processes (BP), cellular components (CC), and molecular functions (MF) to elucidate the key biological activities involved. Additionally, we performed KEGG pathway enrichment analysis to pinpoint significant pathways associated with these targets, applying a false discovery rate (FDR) threshold of < 0.05 to emphasize the most pertinent toxicity pathways. To aid in the interpretation and presentation of our findings, we employed visual analysis for both the GO and KEGG results.

PPI network construction: unveiling target interactions

The STRING database (URL: https://string-db.org/) was used to construct a protein-protein interaction (PPI) network for TDCPP-induced pterygium targets, specifying 'Homo sapiens' and a minimum interaction score of 0.40. Subsequently, the PPI network was imported into Cytoscape3.10.2 software, where the network analyzer plugin was utilized for topological analysis. The genes are ranked by their degree of connectivity. The common targets were analyzed using the cytoscape3.10.2 software MCODE plugin to cluster genes and visually represent target interactions.

Transcriptome sequencing of clinical pterygium tissue

The research protocol was approved by the Ethics Review Committee of the Affiliated Hospital of Yunnan University (approval number 2022198), and all participants gave written informed consent following the Declaration of Helsinki. A surgeon performed all surgical procedures under local anesthesia, with 34 patients undergoing elective pterygium surgery to remove the pterygium tissue and surrounding loose conjunctiva. We used an Agilent 2100 Bioanalyzer to assess the integrity of total RNA extracted from pterygium and bulbar conjunctiva samples. The study data are accessible in the NCBI Sequence Read Archive (SRA) under accession number PRJNA1147595.

WGCNA: Building and analyzing gene co-expression networks

We applied weighted gene co-expression network analysis (WGCNA) to build gene expression networks using the PRJNA1147595 dataset. Our objective was to create a scale-free topology, where the network exhibits a power-law distribution in node connectivity. To determine the best soft threshold for defining gene adjacencies, we used the "pickSoftThreshold" function from the WGCNA package in R program. Subsequently, the adjacency matrix was converted into a topological overlap matrix (TOM), which served as the basis for hierarchical clustering, utilizing dissimilarity measures derived from TOM. For identifying co-expressed gene modules, we employed the dynamic tree-cutting algorithm, setting a minimum module size of 30 genes. This technique allowed us to classify genes into distinct modules based on their expression patterns. To assess the association between these gene modules and pterygium, we examined gene significance (GS) and module membership (MM) metrics. GS reflects the correlation between gene expression and pterygium, while MM gauges the degree of co-expression among genes within a module. By combining GS and MM scores, we pinpointed key modules linked to pterygium, suggesting their potential functional importance in the disease.

Analysis of expression of hub gene in pterygium

The gene sets identified as significant difference modules through WGCNA analysis intersected with the targets of TDCPP-induced pterygium. The genes present in this intersection were considered hub genes. To quantitatively analyze the differential expression of genes in pterygium tissues versus conjunctiva control tissues, we utilized our proprietary sequenced pterygium transcriptome data. Gene expression scatter plots were created with the R package ggplot2 to visually depict expression level distributions across various sample types. Samples were categorized into "pterygium" and "conjunctiva" groups for comparative analysis. Wilcoxon rank-sum tests were used to evaluate expression level differences, yielding corresponding p-values.

Molecular docking: exploring Ligand-Receptor interactions

We ascertained the names, molecular weights, and 2D structures of the active compounds. The 3D structures of the proteins were retrieved from PubChem (URL: https://pubchem.ncbi.nlm.nih.gov/) and UniProt (URL: https://www.uniprot.org/) databases. We then prepared the ligands and proteins for molecular docking with AutoDock online software (URL: https://cadd.labshare.cn/cb-dock2/php/blinddock.php). The crystal structures of the target proteins were refined by eliminating water molecules, adding hydrogen atoms, altering amino acids, optimizing energy levels, and fine-tuning force field settings. Afterward, we conducted a virtual docking screening using Vina in the PyRx software. The Binding Affinity value (in kcal/mol), which measures the strength of ligand-receptor interactions, was used to gauge binding stability, with lower values denoting stronger binding. For further analysis, we utilized Discovery Studio, and PYMOL was employed for visualization purposes. The protein under investigation bore the accession number MMP3 (P08254).

Molecular dynamics simulation

We conducted molecular dynamics (MD) modeling of the TDCPP-MMP3 protein-ligand complex utilizing the Gromacs 2024.1 computational suite (URL: https://www.gromacs.org/)[26,27]. The ligand molecules underwent preprocessing via AmberTools 22, employing the Generalized Amber Force Field (GAFF) parameterization scheme. This preparation involved hydrogen atom addition, calculation of restrained electrostatic potential (RESP) charges using Gaussian 16 W, and integration of the derived charge parameters into the system topology files. The simulations were executed under constant temperature (300 K) and pressure (1 bar) conditions, spanning a total trajectory duration of 100 nanoseconds. The Amber99sb-ildn force field was selected for

molecular interactions, with the system solvated using the TIP3P explicit water model. System stabilization was achieved through initial steepest-descent energy minimization followed by thermal/pressure equilibration phases before production MD runs. Trajectory snapshots sampled every 10 ps were subjected to structural analysis using root mean square deviation (RMSD), root mean square fluctuation (RMSF), radius of gyration (Rg), and hydrogen bonding network assessments[28,29].

Immortalization of human conjunctival fibroblasts

Given that the primary pathological characteristic of pterygium is the hyperplasia of conjunctival fibroblasts. To investigate the impact of TDCPP on the pathogenesis of pterygium, we established immortalized conjunctival fibroblasts for in vitro cellular experiments. Subepithelial fascial tissues of the bulbar conjunctiva, excised from three patients with conjunctivochalasis, were obtained. The tissue specimens were then minced into small squares with side lengths of approximately 0.1 cm. The culture medium was replaced every three days. Once the cells growing around the tissue fragments reached confluence, the tissue fragments were removed. The cells were subsequently digested with trypsin and subcultured into new flasks. The cells were transfected with a lentiviral vector overexpressing Simian Virus 40 (SV40) large T antigen. Puromycin was used for cell selection. The selected cells, designated as passage 1 (P1), were further expanded. Immortalized conjunctival fibroblasts were obtained after at least 13 passages of expansion. At the same time, we performed immunofluorescence staining on the marker Vimentin of the conjunctival fibroblasts to confirm the nature of the cells. We utilized primary conjunctival fibroblasts. Before lentiviral transfection, the cells were observed to grow uniformly in the culture dish. After transfection with the SV40 virus and selection using Puromycin, the cells were found to grow normally. Upon staining with the marker protein Vimentin, which is specific to conjunctival fibroblasts, it was evident that the immortalized fibroblasts uniformly expressed the marker gene. At the same time, we also conducted STR genotyping tests on the constructed cells to clarify the source of the cells.

CCK-8 and RT-qPCR assays: assessing TDCPP effects on fibroblasts

Conjunctival fibroblasts were exposed to varying concentrations of TDCPP (0.5, 1, 1.5, 5, and 50 μM) in the culture medium. The experimental groups included TDCPP-treated concentrations (0.5, 1, 1.5, 5, and 50 μM) and an untreated control group. Fibroblasts from each group were seeded in 12-well plates at a density of 10^5 cells/well with 2 mL of medium and incubated at 37 °C with 5% CO_2 for 24 h. CCK-8 reagent (Proteintech, USA) was added (200 μL/well) and incubated for an additional hour. Absorbance was measured at 450 nm using a microplate reader (BioTek, USA800TS). For RT-qPCR analysis, fibroblasts cultured in dishes were lysed with TRIzol reagent (Thermo Fisher, USA). Total RNA was extracted using a total RNA Extraction Kit (Vazyme, Nanjing, China), and cDNA was synthesized using a cDNA First-Strand Synthesis Kit (TaKaRa, Japan). Gene expression was quantified using TB Green Fast qPCR Mix (TaKaRa, Japan) and normalized to GAPDH using the $2^{-}\Delta\Delta Ct$ method.

Statistical analysis

Version 4.2.1 of the R software is used for data visualization, including enrichment analysis, WCGNA analysis, and group comparison chart drawing, etc. The results are reported as the mean ± standard deviation (SD). For comparing two samples, the Student's t-test was employed to ascertain whether there was a statistically significant difference between groups subjected to different treatments. A p-value of less than 0.05 was considered statistically significant. In the graphical representations, asterisks are utilized to denote the statistical significance of the values. Specifically, *: $P < 0.05$; **: $P < 0.01$; ***: $P < 0.001$.

Results

Chemical characteristics of TDCPP

TDCPP is an organophosphorus compound with the molecular formula C9H15Cl6O4P and a molecular weight of 430.905 g/mol, featuring a phosphate group attached to three 1,3-dichloropropyl groups. Physically, TDCPP appears as a colorless to light yellow, viscous liquid. It is soluble in organic solvents such as alcohols, benzene, and carbon tetrachloride while exhibiting slight solubility in water (0.01% by weight at 30 °C). At 25 °C, it has a density of 1.5 ± 0.1 g/cm³, a melting point of -64 °C, and a boiling point of 457.4 ± 40.0 °C at 760 mmHg. The flash point of TDCPP is 377.7 ± 35.0 °C, and it has a refractive index of 1.497. Additionally, TDCPP is known for its good hydrolytic stability and low volatility, making it a commonly used flame retardant in various materials. The chemical characteristics of TDCPP, including its chemical formulas, molecular weights, and SMILES structures.

Identification of TDCPP-associated targets

After integrating and deduplicating data sourced from Super-Pred, ChEMBL, STITCH, and PharmMapper[21], we identified a total of 273 unique target proteins associated with TDCPP (Fig. 2A). These target proteins are potential molecular targets through which TDCPP exposure may elicit its toxicological effects, potentially increasing the risk of pterygium development. Further investigation and validation of these targets are essential for elucidating the underlying mechanisms and developing strategies to mitigate the adverse ocular surface health effects linked to TDCPP exposure.

Intersection of TDCPP targets with Pterygium-Related genes

1078 pterygium-related target genes were retrieved from the literature, Genecard, and OMIM database. By intersecting these genes with the target genes of TDCPP, we identified 43 shared genes, as illustrated in Fig. 2B. These 43 genes are potential targets implicated in TDCPP-induced pterygium development. Further investigation is necessary to elucidate the specific roles of these genes in pterygium pathogenesis and to assess their potential as therapeutic targets or biomarkers for evaluating the risk of pterygium associated with TDCPP exposure.

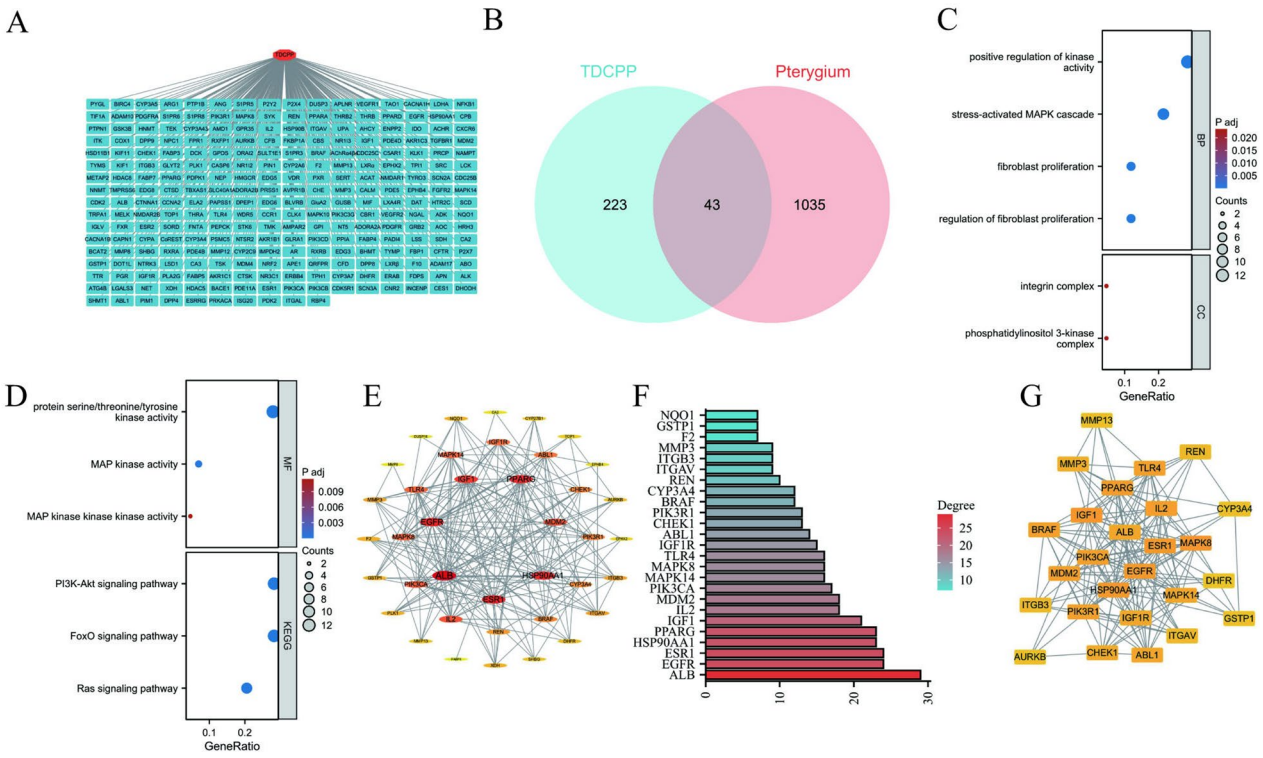

Fig. 2. Identification of TDCPP Targets and GOKEGG Enrichment Analysis. **A**. By integrating data from Super-Pred, ChEMBL, STITCH, and PharmMapper, a total of 273 unique target proteins associated with TDCPP were identified. **B**. An intersection analysis was conducted between 1078 pterygium-related target genes and the target genes of TDCPP. **C**-**D**. The results of GO functional enrichment analysis are presented in the Biological Process (BP), Cellular Component (CC), and Molecular Function (MF) categories. The results of KEGG pathway enrichment analysis are displayed. **E**-**F**. The PPI network consists of 39 nodes and 220 edges, with a bar graph representing the PPI. **G**. The result of the MCODE cluster module analysis is presented.

Enrichment analysis of gene ontology and KEGG pathways

We performed a Gene Ontology (GO) analysis on 43 potential targets using the R project, with a particular emphasis on the Homo sapiens species. The GO terms were sorted based on their false discovery rate (FDR) values. For visualization purposes, we selected the most relevant terms from each of the Biological Process (BP), Cellular Component (CC), and Molecular Function (MF) categories, which exhibited the lowest FDR values, to be displayed in enrichment analysis plots. The BP terms that were enriched included 'positive regulation of kinase activity (GO:0033674)', 'stress-activated MAPK cascade (GO:0051403)' and 'regulation of fibroblast proliferation (GO:0048145)' and 'fibroblast proliferation (GO:0048144)' (Fig. 2C). Additionally, CC terms such as 'phosphatidylinositol 3-kinase complex (GO:0005942)', 'integrin complex (GO:0008305)' (Fig. 2C). MF terms such as 'protein serine/threonine/tyrosine kinase activity (GO:0004712)', 'MAP kinase activity (GO:0004707)' and 'MAP kinase kinase kinase activity (GO:0004709)' were also enriched (Fig. 2D). We utilized the 'clusterProfiler' R package for KEGG analysis on the 43 potential targets to clarify their roles in specific signaling pathways. We generated statistical bubble plots and categorical histograms to visually represent the relevant KEGG signaling pathways (Fig. 2D). GO and KEGG analyses indicated that these genes are widely distributed and expressed across different subcellular locations, with significant involvement in signaling pathways, particularly the FoxO signaling pathway and those associated with fluid shear stress and atherosclerosis. Notably, among the enriched KEGG signaling pathways, those associated with PI3K-Akt signaling pathway and Ras signaling pathway were prominently featured.

PPI network construction and MCODE cluster analysis

We utilized the STRING database to construct a Protein-Protein Interaction (PPI) network for the 43 overlapping targets, which was subsequently visualized with Cytoscape3.10.2. This PPI network consisted of 39 nodes and 220 edges. Additionally, we generated a bar graph depicting the PPI using R software, as illustrated in Fig. 2E **and F**. Moreover, we imported the 43 shared targets of TDCPP and pterygium into the Metascape database to perform MCODE cluster module analysis, with the hub genes presented in Fig. 2G.

WGCNA analysis of gene co-expression modules

We applied the WGCNA algorithm to create co-expression modules based on expression data from 34 pterygium and 34 conjunctiva samples. For in-depth analysis, we focused on the top quartile of genes exhibiting the highest variability. Sample clustering was executed using the "WGCNA" package, with the outcomes presented in

Fig. 3A. At a power value of 10, we achieved an independence level of 0.9 and improved mean connectivity, as shown in Fig. 3B and C. By employing the dynamic tree-cut approach, we discovered ten distinct gene co-expression modules in pterygium. Furthermore, a heatmap of the Topological Overlap Matrix (TOM) was produced for visualization purposes (refer to Fig. 3D and E). The genes within these modules were then utilized to investigate the association between module eigengenes and clinical traits. A total of 3910 genes were assigned to ten modules, among which the tan module (correlation coefficient = -0.66, $P = 1e\text{-}9$) and the salmon module (correlation coefficient = 0.78, $P = 7e\text{-}15$) demonstrated significant associations with the pterygium phenotype (Fig. 3F).

Intersection of target gene and expression in pterygium

Forty-three genes were found to be common between TDCPP target genes and pterygium-associated target genes. A Venn diagram was created to illustrate the relationships among these 43 overlapping targets and the tan and salmon modules determined through Weighted Gene Co-expression Network Analysis (Fig. 4A). We pinpointed the *MMP3* gene as pivotal in the development of pterygium following TDCPP exposure. Our results indicate a notable difference in *MMP3* gene expression levels between conjunctival and pterygium samples, with *MMP3* expression significantly upregulated in pterygium tissues (Fig. 4B). This altered expression pattern hints at specific pathways that could be promising therapeutic targets.

Molecular Docking and dynamics simulations of TDCPP with MMP3

The *MMP3* gene has undergone molecular docking simulations with TDCPP, and the most probable binding conformations are depicted in Fig. 5A. This figure illustrates the docking results, revealing that TDCPP binds to a specific site on MMP3. Figure 5B presents the amino acids at the binding site, which primarily interact with TDCPP through hydrogen bonds. A lower binding energy between the ligand and receptor indicates a higher likelihood of interaction. Specifically, the binding energy of TDCPP with MMP3 was found to be -5.9 kcal/mol, as shown in Fig. 5C.

Although the molecular docking analysis employed a semi-flexible docking protocol, this approach failed to account for the inherent flexibility of the protein structure, as well as thermodynamic effects including

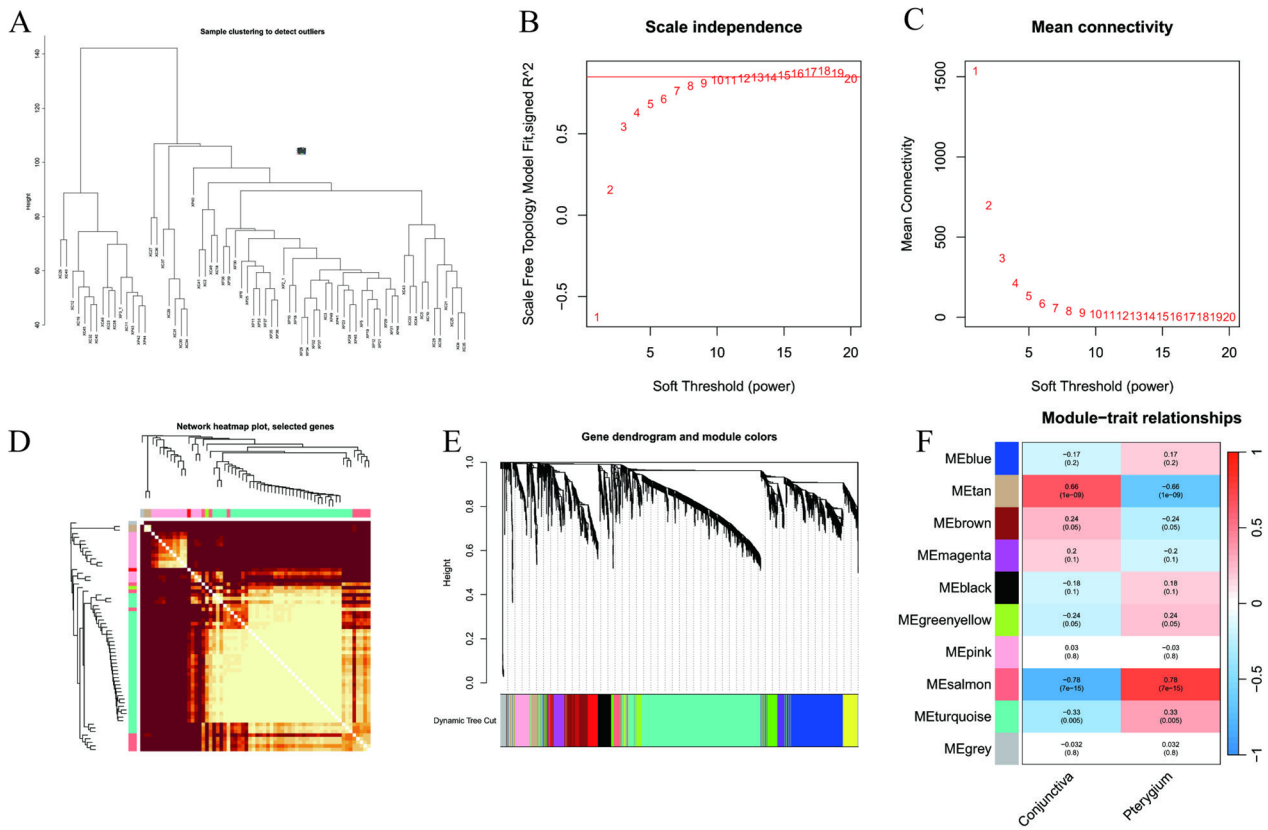

Fig. 3. Weighted Gene Co-expression Network Analysis (WGCNA) for Screening Target Module Genes. **A**. The gene clustering tree is shown. **B**-**C**. The relevant parameters for WGCNA network construction are provided, with a power value of 10 achieving an independence level of 0.9. **D**. A clustering heat map of all module genes in the WGCNA analysis is displayed. **E**. A heat map illustrating the correlation between different phenotypes and modules based on WGCNA analysis is presented. **F**. The expression of the salmon and turquoise module genes in the two groups is shown through a cluster heat map, where red represents high gene expression and blue represents low gene expression.

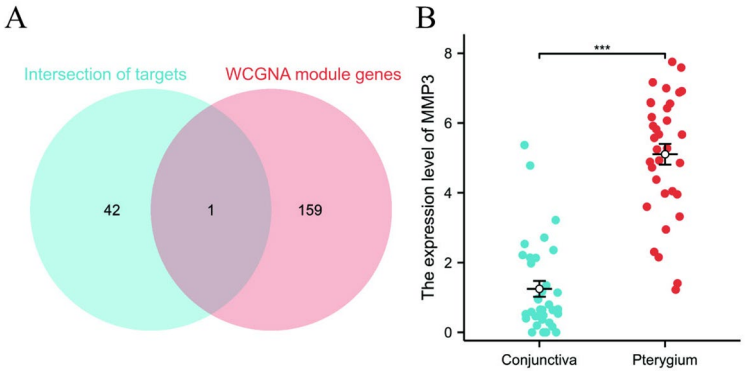

Fig. 4. Intersection of Target Genes and Their Expression in Pterygium. **A**. A Venn diagram depicts the relationships among the 43 intersecting targets and the tan and salmon modules identified through WGCNA. **B**. The expression of *MMP3* was significantly elevated in pterygium tissues.

temperature, pressure, and solvent interactions. To further investigate the stability of protein-ligand interactions, we performed molecular dynamics (MD) simulations of the TDCPP-MMP3 complex. The structural stability of the protein before and after ligand binding was evaluated by calculating the root mean square deviation (RMSD) of backbone atoms, which provides quantitative information about structural fluctuations throughout the MD trajectory. The RMSD values for the TDCPP-MMP3 complex exhibited a gradual increase before reaching a plateau after 20 ns of simulation, indicating the formation of a stable protein-ligand complex. The average RMSD values were 0.119 ± 0.011 nm for the protein alone and 0.134 ± 0.009 nm for the protein-ligand complex (Fig. 5D). To elucidate how ligand binding influences the flexibility of amino acid residues during simulation, we analyzed the root mean square fluctuation (RMSF). Our RMSF analysis revealed comparable residue fluctuations between the protein-only and complex systems. Notably, residues within the 145–160 region exhibited the most significant fluctuations, with amino acids near position 160 constituting the protein-ligand binding site. This observation suggests that ligand binding stabilizes the conformational dynamics of residues within the protein's active site (Fig. 5E). The average radius of gyration (Rg) values was 1.517 ± 0.005 nm for the protein and 1.518 ± 0.005 nm for the complex, indicating nearly identical compactness between the two systems (Fig. 5F). The solvent-accessible surface area (SASA) values also demonstrated remarkable similarity, with averages of 90.198 ± 1.434 nm^2 and 90.028 ± 1.490 nm^2 for the protein and complex, respectively. The absence of significant SASA fluctuations throughout the simulation suggests that both systems achieved thermodynamic equilibrium (Fig. 5G). Based on our analysis, the protein-ligand complex formed an average of 0.443 ± 0.498 hydrogen bonds during the 100 ns simulation period (Fig. 5H).

CCK-8 and QPCR results on conjunctival fibroblasts exposed to TDCPP

We introduced TDCPP at various concentrations (0.5, 1, 1.5, 5, and 50 μM) into the culture dishes. It was observed that at low concentrations, the growth status of the cells showed no significant difference compared to the control group (Fig. 6A). However, when the concentration reached 50 μM, the growth of fibroblasts was inhibited. The cells exhibited a rounded morphology, and inter-cellular connections became less prominent (Fig. 6A). The results from the CCK-8 assay demonstrated that after culturing conjunctival fibroblasts for 24 h and then exposing them to different concentrations of TDCPP (0.5, 1, 1.5, 5, and 50 μM) in the culture medium. After continuous exposure to different concentrations of TDCPP for 24 h, all the cells were collected for the CCK-8 assay. Culturing conjunctival fibroblasts under 0.5 μM and 1 μM conditions could enhance their viability, while viability decreased under 50 μM conditions. These findings revealed a notable increase in cell viability at the 0.5 μM concentration, suggesting that exposure to low-concentration TDCPP might induce the proliferation of conjunctival fibroblasts (Fig. 6B). Because the cell activity increased most significantly after treatment with 0.5 μM concentration of TDCPP, the cells treated with this concentration were selected for the subsequent experiments. Meanwhile, we observed that under 0.5 μM TDCPP exposure, the expression level of the *MMP3* gene in conjunctival fibroblasts of the experimental group was significantly increased compared with that in the control group (Fig. 6C). We hypothesize that exposure of conjunctival tissue to TDCPP may potentially promote the onset of pterygium. The underlying mechanism is likely dependent on the up-regulation of the *MMP3* gene in fibroblasts, which subsequently facilitates cell proliferation.

Discussion

This study highlights the health risks associated with Tris(1,3-dichloro-2-propyl) phosphate (TDCPP) exposure, particularly its role in pterygium development through changes in gene expression. Pterygium, an abnormal tissue growth on the conjunctiva, can impair vision and cause discomfort, significantly reducing quality of life[3,7]. Although surgical excision is a viable treatment option, the recurrence of pterygium poses a considerable challenge, necessitating deeper exploration into its underlying mechanisms and associated risk factors[5,7]. TDCPP is a prevalent organophosphate flame retardant renowned for its effectiveness and low volatility (Zhong et al., 2020). Elucidating the mechanisms through which TDCPP interacts with cellular processes is vital for assessing its safety profile[30]. This study offers valuable insights into the disruptive effects of TDCPP exposure

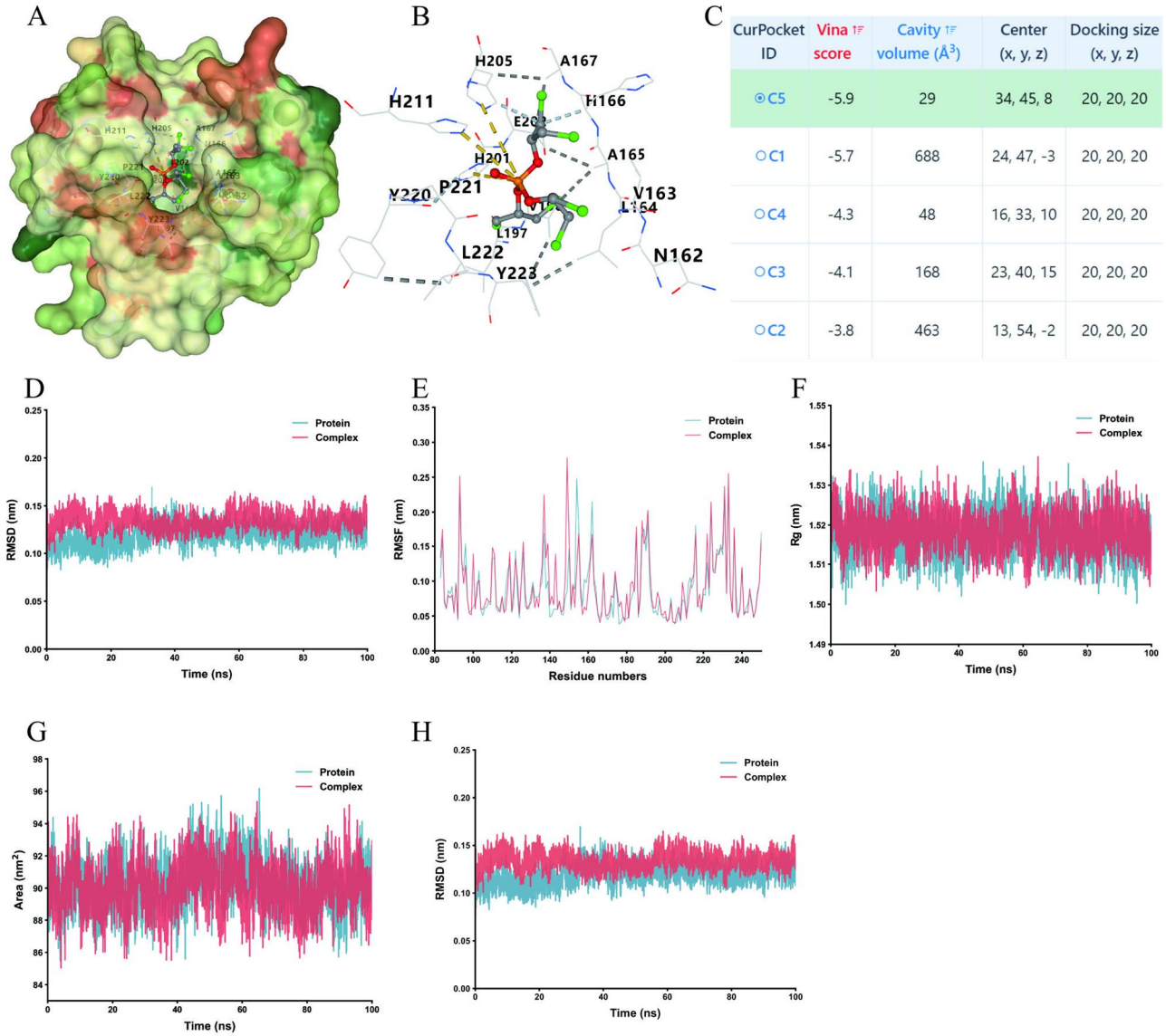

CurPocket ID	Vina score	Cavity volume (Å³)	Center (x, y, z)	Docking size (x, y, z)
◉C5	-5.9	29	34, 45, 8	20, 20, 20
○C1	-5.7	688	24, 47, -3	20, 20, 20
○C4	-4.3	48	16, 33, 10	20, 20, 20
○C3	-4.1	168	23, 40, 15	20, 20, 20
○C2	-3.8	463	13, 54, -2	20, 20, 20

Fig. 5. Molecular docking and Molecular dynamics result analysis. **A**. The probable binding conformations of TDCPP-MMP3 are shown. **B**. The binding of TDCPP to surrounding amino acids is illustrated. **C**. The binding energy of TDCPP with MMP3 is presented. **D**. RMSD plot comparing the structural dynamics of the protein-only system (blue trace) and the TDCPP-MMP3 protein-ligand complex (red trace) throughout the molecular dynamics simulation. **E**. RMSF plot illustrating the residue-specific flexibility profiles of the TDCPP-MMP3 complex. **F**. Rg plot demonstrating the compactness evolution of the TDCPP-MMP3 complex during the simulation. **G**. SASA plot depicting the temporal changes in surface exposure of the protein-ligand complex, reflecting conformational adjustments and solvent interactions. **H**. H-bond count plot quantifying the number of intermolecular hydrogen bonds formed between the TDCPP ligand and MMP3 protein residues during the molecular dynamic trajectory.

on normal cellular functions, potentially leading to detrimental outcomes like the development of pterygium. The research findings highlight the urgency of assessing the long-term health implications of TDCPP, especially among populations with substantial exposure, to guide regulatory policies and public health interventions.

The enrichment analysis unveiled that the target genes linked to TDCPP primarily engage in the FoxO signaling pathway (Fig. 2D), implying their potential involvement in the etiology of pterygium. This pathway is pivotal for governing cellular processes, including apoptosis, cell cycle progression, and oxidative stress response, all of which are essential for preserving cellular homeostasis and warding off tumorigenesis[31,32]. The implication of this pathway hints that TDCPP might affect pterygium development through mechanisms that regulate these crucial cellular functions. The overlap between TDCPP-related target genes and pterygium-associated genes underscores the significance of these pathways in deciphering the molecular mechanisms driving pterygium pathogenesis. Grasping these pathways may ultimately pave the way for enhanced diagnostic and therapeutic strategies for managing pterygium and related ocular disorders.

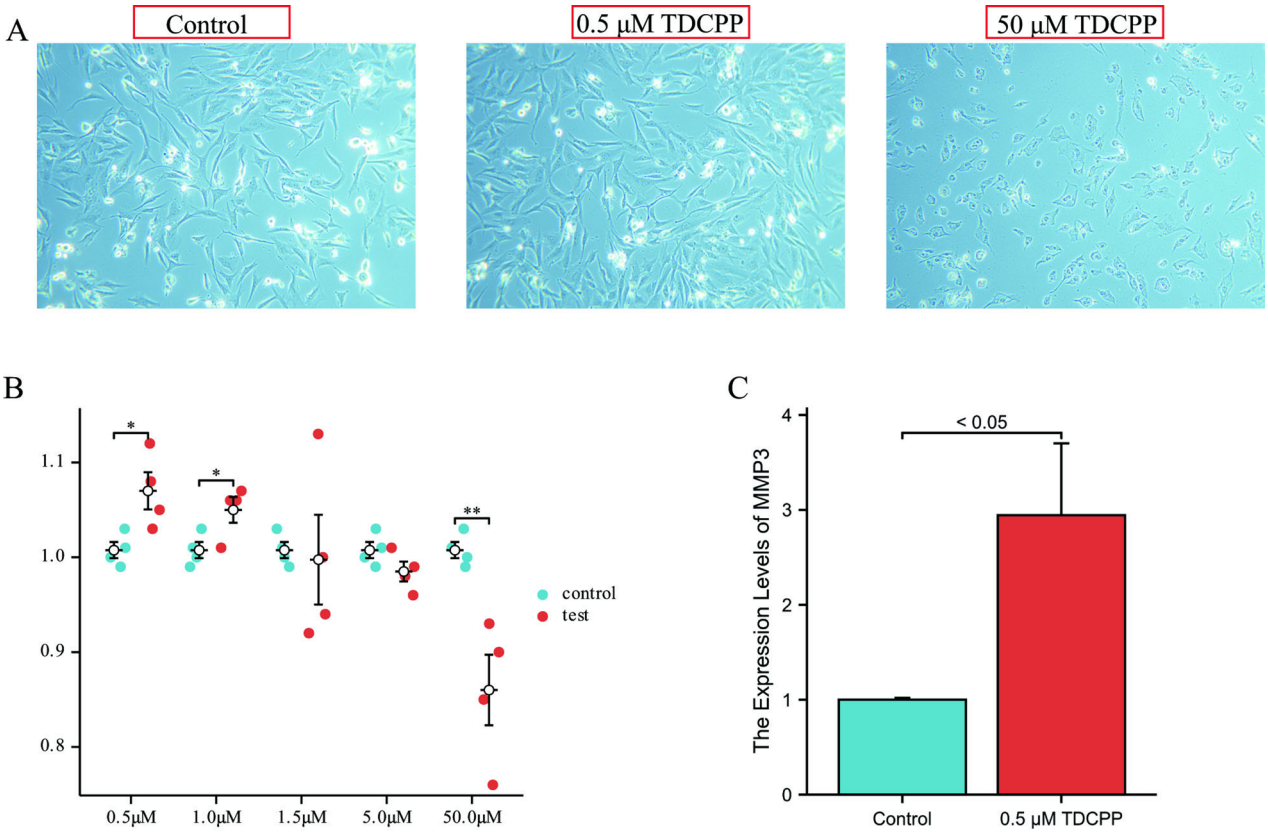

Fig. 6. Results of cell morphology, cell viability assay, and MMP3 expression after TDCPP exposure.**A**. Growth morphology of the control group cells. **B**. Cell growth morphology in the 0.5 μM TDCPP exposure group. **C**. Cell growth morphology in the 50 μM TDCPP exposure group. **D**. The results of the CCK – 8 assay. TDCPP (0.5, 1, 1.5, 5, and 50 μM) in the culture medium, culturing conjunctival fibroblasts under 0.5 μM and 1 μM conditions could enhance their viability, while viability decreased under 50 μM conditions. **E**. Under 0.5 μM TDCPP exposure, the expression level of the *MMP3* gene in conjunctival fibroblasts of the experimental group was significantly increased compared with that in the control group.

WCGNA analysis and the intersection of genes involved in pterygium pathogenesis and TDCPP targets revealed that the matrix metalloproteinase 3 (MMP3) gene is pivotal in pterygium development, particularly under TDCPP exposure. Elevated *MMP3* expression levels in pterygium tissues (Fig. 4B) indicate its involvement in the remodeling of the extracellular matrix (ECM), which is vital for maintaining tissue integrity and function[33,34]. *MMP3* is recognized for its ability to degrade various ECM components, thereby influencing cellular processes such as proliferation and migration, which are central to pterygium development[34,35]. Additionally, *MMP3* has been shown to modulate inflammatory responses, often linked to pterygium formation, by regulating cytokines and chemokines that drive inflammatory processes, thus associating it with the chronic inflammation observed in pterygium patients[33]. Our observations align with previous findings, showing significantly elevated *MMP3* expression in pterygium tissues relative to normal conjunctival tissues[36], indicating its potential as a biomarker for pterygium severity and a therapeutic target. The evidence collectively supports the hypothesis that *MMP3* plays a crucial role in pterygium pathogenesis and represents a promising target for therapeutic strategies to mitigate the adverse effects of TDCPP exposure and pterygium development.

To figure out the deeper molecular mechanism, molecular docking studies have been conducted to investigate the interaction between TDCPP and *MMP3*, revealing a binding energy of -5.9 kcal/mol, indicative of a strong affinity between the two molecules. Given that, we hypothesized that TDCPP may contribute to the development of pterygium via its interaction with MMP3. Molecular dynamics indicate the formation of a stable TDCPP-MMP3 protein-ligand complex and both systems achieved thermodynamic equilibrium (Fig. 5D-G). To validate this hypothesis, the detrimental effects of TDCPP on immortalied human conjunctival fibroblasts were carried out to figure out the pterygium pathogenesis. The experimental results from our CCK-8 assay further corroborate the in silico findings, demonstrating that low concentrations (0.5 and 1.0 μM) of TDCPP can enhance the proliferation of conjunctival fibroblasts through the upregulation of the *MMP3* gene. This finding suggests a potential link between TDCPP exposure and the cellular mechanisms underlying pterygium development. The dose-dependent effects observed in our study highlight the need for further research into the cellular response to varying concentrations of TDCPP, particularly regarding its potential to promote fibroblast proliferation and migration in ocular tissues. Our results are consistent with prior research emphasizing the importance of MMPs in various pathological conditions, such as cancer and tissue remodeling, suggesting that TDCPP's modulation

of MMP3 could disrupt these processes[34,36–38]. Additionally, molecular dynamics simulations offer further insights into the temporal stability and dynamics of the TDCPP-MMP3 complex. These simulations aim to assess conformational changes and atomic-level interactions, providing a more comprehensive understanding of the binding mechanism. Previous studies have shown that molecular dynamics can uncover crucial information about ligand-receptor interactions, including key residues involved in binding and the complex's stability under physiological conditions[39,40]. These findings emphasize the need for further validation experiments, including in vivo assays and functional studies, to confirm the biological relevance of the TDCPP-MMP3 interaction and its implications for pterygium development. These validation efforts will improve our understanding of TDCPP's molecular toxicology and may inform future therapeutic strategies to mitigate exposure risks.

This study emphasizes the significance of elucidating the molecular mechanisms underlying TDCPP-induced pterygium. We speculate that the potential mechanisms underlying the upregulation of MMP3 expression caused by TDCPP treatment may involve the following two aspects: The binding of TDCPP to MMP3 may enhance its activity through allosteric effects and trigger the upregulation of expression[41]. TDCPP may indirectly regulate the upregulation of MMP3 expression by influencing the cell proliferation signaling pathway[42]. The limitation of this study primarily revolves around the relatively small sample size and the absence of clinical validation, which restricts the generalizability of the findings. While bioinformatics analyses have successfully identified potential target genes and pathways involved in the pathogenesis of pterygium related to TDCPP exposure, the lack of extensive in vivo or clinical data hinders a comprehensive understanding of the disease mechanisms. Moreover, the integration of wet laboratory experiments with bioinformatics results is insufficient, necessitating further studies to solidify the biological relevance of our findings. Future research should aim to incorporate larger cohorts and diverse populations to confirm the identified associations and enhance the translational potential of our results.

This study has identified significant molecular targets and pathways linked to TDCPP-induced pterygium, with a particular emphasis on the MMP3 gene as a promising biomarker and therapeutic target. Our findings enhance the understanding of the underlying molecular mechanisms in pterygium pathogenesis and underscore the necessity of investigating these targets for the development of future therapeutic strategies. Follow-up study should be done to confirm these results and evaluate the potential clinical significance of targeting MMP3 and its associated pathways in alleviating the health effects of TDCPP exposure.

Limitation

The limited sample size of clinical pterygium tissues may restrict the generalizability of our results, highlighting the need for larger cohorts to establish robust correlations. Additionally, potential batch effects stemming from the heterogeneous datasets used in bioinformatics analyses may introduce variability. We conducted the experiments using pure TDCPP substance instead of environmental samples. The real-world exposure involves a mixture of chemicals, matrix effects, and bioavailability factors that are not replicated in our in vitro model. Collectively, these factors underscore the importance of conducting further investigations employing diverse methodologies and larger population samples to validate the identified molecular targets and elucidate their roles in pterygium development.

Conclusion

This study has identified significant molecular targets and pathways linked to TDCPP-induced pterygium, with a particular emphasis on the *MMP3* gene as a promising biomarker and therapeutic target. Our findings enhance the understanding of the underlying molecular mechanisms in pterygium pathogenesis and underscore the necessity of investigating these targets for the development of future therapeutic strategies. Ongoing research is crucial to confirm these results and evaluate the potential clinical significance of targeting MMP3 and its associated pathways in alleviating the health effects of TDCPP exposure.

Data availability

Data will be made available on request. Our RNA-seq data have been deposited in Sequence Read Archive (SRA) with accession numbers PRJNA1147595. For those interested in accessing the data from this study, we kindly request that you contact the corresponding author, Hai Liu.

Received: 19 June 2025; Accepted: 28 October 2025
Published online: 07 November 2025

References

1. Alqahtani, J. M. The prevalence of pterygium in alkhobar: A hospital-based study. *J. Fam. Commun. Med.* **20**, 159–161. https://doi.org/10.4103/2230-8229.121980 (2013).
2. Rezvan, F. et al. Prevalence and risk factors of pterygium: a systematic review and meta-analysis. *Surv. Ophthalmol.* **63**, 719–735. https://doi.org/10.1016/j.survophthal.2018.03.001 (2018).
3. Akbari, M. Update on overview of pterygium and its surgical management. *J. Popul. Ther. Clin. Pharmacol. = J. De la. Therapeutique Des. Populations Et De la. Pharmacologie Clinique.* **29**, e30–e45. https://doi.org/10.47750/jptcp.2022.968 (2022).
4. Thompson, J. P. et al. Comparison of pterygium recurrence rates between attending physicians and supervised trainee residents. *Cornea* **41**, 12–15. https://doi.org/10.1097/ico.0000000000002721 (2022).
5. Alsarhani, W. et al. Characteristics and recurrence of pterygium in Saudi arabia: a single center study with a long follow-up. *BMC Ophthalmol.* **21**, 207. https://doi.org/10.1186/s12886-021-01960-0 (2021).
6. Lu, C. W. et al. Impacts of air pollution and meteorological conditions on dry eye disease among residents in a Northeastern Chinese metropolis: a six-year crossover study in a cold region. *Light Sci. Appl.* **12**, 186. https://doi.org/10.1038/s41377-023-01207-1 (2023).

7. Hill, J. C. & Maske, R. Pathogenesis of pterygium. *Eye (London England)*. **3** (Pt 2), 218–226. https://doi.org/10.1038/eye.1989.31 (1989).
8. Yang, D. L. et al. Indoor air pollution and human ocular diseases: associated contaminants and underlying pathological mechanisms. *Chemosphere* **311**, 137037. https://doi.org/10.1016/j.chemosphere.2022.137037 (2023).
9. Liu, H. et al. Degradation of tris(2-chloroethyl) phosphate (TCEP) by thermally activated persulfate: combination of experimental and theoretical study. *Sci. Total Environ.* **809**, 152185. https://doi.org/10.1016/j.scitotenv.2021.152185 (2022).
10. Meeker, J. D. & Stapleton, H. M. House dust concentrations of organophosphate flame retardants in relation to hormone levels and semen quality parameters. **118**, 318–323, doi: (2010). https://doi.org/10.1289/ehp.0901332
11. Xiang, P. et al. Molecular mechanisms of dust-induced toxicity in human corneal epithelial cells: water and organic extract of office and house dust. *Environ. Int.* **92–93**, 348–356. https://doi.org/10.1016/j.envint.2016.04.013 (2016).
12. Araki, A. et al. Phosphorus flame retardants in indoor dust and their relation to asthma and allergies of inhabitants. *Indoor Air*. **24**, 3–15. https://doi.org/10.1111/ina.12054 (2014).
13. Tan, H. et al. Co-Existence of organophosphate Di- and Tri-Esters in house dust from South China and Midwestern united states: implications for human exposure. *Environ. Sci. Technol.* **53**, 4784–4793. https://doi.org/10.1021/acs.est.9b00229 (2019).
14. Zhao, J. Y. et al. A systematic scoping review of epidemiological studies on the association between organophosphate flame retardants and neurotoxicity. *Ecotoxicol. Environ. Saf.* **243**, 113973. https://doi.org/10.1016/j.ecoenv.2022.113973 (2022).
15. Zhou, X. et al. Organophosphate flame retardant TDCPP: A risk factor for renal cancer? *Chemosphere* **305**, 135485. https://doi.org/10.1016/j.chemosphere.2022.135485 (2022).
16. Xiang, P. et al. Effects of organophosphorus flame retardant TDCPP on normal human corneal epithelial cells: implications for human health. *Environ. Pollut.* **230**, 22–30. https://doi.org/10.1016/j.envpol.2017.06.036 (2017).
17. Zhang, Z. N. et al. Effects of TCPP and TCEP exposure on human corneal epithelial cells: oxidative damage, cell cycle arrest, and pyroptosis. *Chemosphere* **331**, 138817. https://doi.org/10.1016/j.chemosphere.2023.138817 (2023).
18. Ke, H. et al. Study on prevalence of pterygium and its influencing factors in rural population in 6 regions of Yunnan Province. *Zhonghuayanke* **58**, 9 (2022).
19. Gupta, M., Arya, S., Agrawal, P., Gupta, H. & Sikka, R. Unravelling the molecular tapestry of pterygium: insights into genes for diagnostic and therapeutic innovations. *Eye* **38**, 2880–2887. https://doi.org/10.1038/s41433-024-03186-y (2024).
20. Seet, L. F., Tong, L., Su, R. & Wong, T. T. Involvement of SPARC and MMP-3 in the Pathogenesis of Human Pterygium. *Investig. Ophthalmol. Vis. Sci.* 53, 587–595 https://doi.org/10.1167/iovs.11-7941 (2012).
21. Wang, X., Pan, C., Gong, J., Liu, X. & Li, H. Enhancing the enrichment of Pharmacophore-Based target prediction for the polypharmacological profiles of drugs. *J. Chem. Inf. Model.* **56**, 1175–1183. https://doi.org/10.1021/acs.jcim.5b00690 (2016).
22. Wang, X. et al. PharmMapper 2017 update: a web server for potential drug target identification with a comprehensive target pharmacophore database. *Nucleic Acids Res.* **45**, W356–w360. https://doi.org/10.1093/nar/gkx374 (2017).
23. Liu, X. et al. PharmMapper server: a web server for potential drug target identification using pharmacophore mapping approach. *Nucleic Acids Res.* **38**, W609–614. https://doi.org/10.1093/nar/gkq300 (2010).
24. Yu, G., Wang, L. G., Han, Y. & He, Q. Y. ClusterProfiler: an R package for comparing biological themes among gene clusters. *Omics: J. Integr. Biology*. **16**, 284–287. https://doi.org/10.1089/omi.2011.0118 (2012).
25. Kanehisa, M., Furumichi, M., Sato, Y., Matsuura, Y. & Ishiguro-Watanabe, M. KEGG: biological systems database as a model of the real world. *Nucleic Acids Res.* **53**, D672–d677. https://doi.org/10.1093/nar/gkae909 (2025).
26. Abraham, M. J. et al. High performance molecular simulations through multi-level parallelism from laptops to supercomputers. *SoftwareX 1–2*. **GROMACS** https://doi.org/10.1016/j.softx.2015.06.001 (2015). 19–25, doi.
27. Van Der Spoel, D. et al. GROMACS: fast, flexible, and free. *J. Comput. Chem.* **26**, 1701–1718. https://doi.org/10.1002/jcc.20291 (2005).
28. Du, S., Zhang, X. X., Gao, X. & He, Y. B. Structure-based screening of FDA-approved drugs and molecular dynamics simulation to identify potential leukocyte antigen related protein (PTP-LAR) inhibitors. *Comput. Biol. Chem.* **113**, 108264. https://doi.org/10.1016/j.compbiolchem.2024.108264 (2024).
29. Yekeen, A. A., Durojaye, O. A., Idris, M. O., Muritala, H. F. & Arise, R. O. CHAPERON < em > g: A tool for automated GROMACS-based molecular dynamics simulations and trajectory analyses. *Comput. Struct. Biotechnol. J.* **21**, 4849–4858. https://doi.org/10.1016/j.csbj.2023.09.024 (2023).
30. Zhong, X. et al. Neonatal exposure to organophosphorus flame retardant TDCPP elicits neurotoxicity in mouse hippocampus via microglia-mediated inflammation in vivo and in vitro. *Arch. Toxicol.* **94**, 541–552. https://doi.org/10.1007/s00204-019-02635-y (2020).
31. Tu, S. & Qiu, Y. Molecular subtypes and scoring tools related to Foxo signaling pathway for assessing hepatocellular carcinoma prognosis and treatment responsiveness. *Front. Pharmacol.* **14**, 1213506. https://doi.org/10.3389/fphar.2023.1213506 (2023).
32. Zhang, M. et al. Astragaloside IV protects against lung injury and pulmonary fibrosis in COPD by targeting GTP-GDP domain of RAS and downregulating the RAS/RAF/FoxO signaling pathway. *Phytomedicine: Int. J. Phytotherapy Phytopharmacology*. **120**, 155066. https://doi.org/10.1016/j.phymed.2023.155066 (2023).
33. Kim, Y. H. et al. Inhibition of pterygium fibroblast migration and outgrowth by bevacizumab and cyclosporine A involves Down-Regulation of matrix Metalloproteinases-3 and – 13. *PloS One*. **12**, e0169675. https://doi.org/10.1371/journal.pone.0169675 (2017).
34. Seet, L. F., Tong, L., Su, R. & Wong, T. T. Involvement of SPARC and MMP-3 in the pathogenesis of human pterygium. *Investig. Ophthalmol. Vis. Sci.* **53**, 587–595. https://doi.org/10.1167/iovs.11-7941 (2012).
35. Zhang, S., Wang, D. & Yan, Z. Increasing of matrix metalloproteinase 3 in bovine endometritis. *Theriogenology* **175**, 83–88. https://doi.org/10.1016/j.theriogenology.2021.09.001 (2021).
36. Kim, Y. H. et al. Cyclosporine A downregulates MMP-3 and MMP-13 expression in cultured pterygium fibroblasts. *Cornea* **34**, 1137–1143. https://doi.org/10.1097/ico.0000000000000477 (2015).
37. Tenlep, S. Y. N. et al. Tris(1,3-dichloro-2-propyl) phosphate is a metabolism-disrupting chemical in male mice. *Toxicol. Lett.* **374**, 31–39. https://doi.org/10.1016/j.toxlet.2022.11.021 (2023).
38. Razavi, P. et al. Matrix Metalloproteinase-3 but not matrix Metalloproteinase-9, implicated in the manifestation of chronic periodontitis. *Rep. Biochem. Mol. Biology*. **11**, 656–662. https://doi.org/10.52547/rbmb.11.4.656 (2023).
39. Wang, X. & Song, F. The neurotoxicity of organophosphorus flame retardant Tris (1,3-dichloro-2-propyl) phosphate (TDCPP): main effects and its underlying mechanisms. *Environ. Pollution (Barking Essex: 1987)*. **346**, 123569. https://doi.org/10.1016/j.envpol.2024.123569 (2024).
40. Liu, X. et al. Effects of long-term exposure to TDCPP in zebrafish (Danio rerio) - Alternations of hormone balance and gene transcriptions along hypothalamus-pituitary axes. *Anim. Models Experimental Med.* **5**, 239–247. https://doi.org/10.1002/ame2.12215 (2022).
41. Xu, T. et al. Bioconcentration, metabolism and alterations of thyroid hormones of Tris(1,3-dichloro-2-propyl) phosphate (TDCPP) in zebrafish. *Environ. Toxicol. Pharmacol.* **40**, 581–586. https://doi.org/10.1016/j.etap.2015.08.020 (2015).
42. Zhang, W. et al. TDCPP protects cardiomyocytes from H(2)O(2)-induced injuries via activating PI3K/Akt/GSK3β signaling pathway. *Mol. Cell. Biochem.* **453**, 53–64. https://doi.org/10.1007/s11010-018-3431-8 (2019).

Acknowledgements

We express our gratitude to the patients who donated their pterygium tissue for this project.

Author contributions

Ji Yang: Writing – original draft, Visualization, Investigation, Conceptualization. Jiajie Li: Writing – original draft, Data curation, Investigation, Validation. Boyu Liang and Nishan Zhao: Writing – original draft, Visualization, Supervision, cell experiment. Peng Zhang: Investigation, collect samples. Chengyan Fang: Investigation, collect samples. Tao Xie: Methodology . Ping Xiang: Writing–review & editing, Supervision, Conceptualization. Hai Liu: Writing–review & editing, Supervision, Project administration, Methodology, Funding acquisition, and Conceptualization.

Funding

This work was carried out with the support of the National Natural Science Foundation of China (Grant No. 82460201). Yunnan University Medical Research Foundation (YDYXJJ2024-0003). Key Project of the Provincial Clinical Medical Center of Yunnan Province (2024YNLCYXZX0343). Yunnan Young and middle-aged Academic and Technical Leader Project (Grant No. 202205AC160016), National Clinical Key Specialty Ophthalmology Open Foundation (Grant No. ZKF2024041 and ZKF2024042) and the Yunnan Xingdian Youth Talent Program (YNQR-QNRC-2018-049, XDYC-MY-2024).

Declarations

Competing interests

The authors declare no competing interests.

Ethics declarations

The research protocol was approved by the Ethics Review Committee of the Affiliated Hospital of Yunnan University (approval number: 2022198), and all study participants provided written informed consent.

Additional information

Supplementary Information The online version contains supplementary material available at https://doi.org/10.1038/s41598-025-26338-w.

Correspondence and requests for materials should be addressed to P.X. or H.L.

Reprints and permissions information is available at www.nature.com/reprints.

Publisher's note Springer Nature remains neutral with regard to jurisdictional claims in published maps and institutional affiliations.